



UNIVERSITY OF LEEDS

This is a repository copy of *An analysis of energy flow in a turbocharged diesel engine of a heavy truck and potentials of improving fuel economy and reducing exhaust emissions*.

White Rose Research Online URL for this paper:
<http://eprints.whiterose.ac.uk/142448/>

Version: Accepted Version

Article:

Gao, J, Chen, H, Tian, G et al. (2 more authors) (2019) An analysis of energy flow in a turbocharged diesel engine of a heavy truck and potentials of improving fuel economy and reducing exhaust emissions. *Energy Conversion and Management*, 184. pp. 456-465. ISSN 0196-8904

<https://doi.org/10.1016/j.enconman.2019.01.053>

© 2019 Elsevier Ltd. All rights reserved. Licensed under the Creative Commons Attribution-Non Commercial No Derivatives 4.0 International License (<https://creativecommons.org/licenses/by-nc-nd/4.0/>).

Reuse

This article is distributed under the terms of the Creative Commons Attribution-NonCommercial-NoDerivs (CC BY-NC-ND) licence. This licence only allows you to download this work and share it with others as long as you credit the authors, but you can't change the article in any way or use it commercially. More information and the full terms of the licence here: <https://creativecommons.org/licenses/>

Takedown

If you consider content in White Rose Research Online to be in breach of UK law, please notify us by emailing eprints@whiterose.ac.uk including the URL of the record and the reason for the withdrawal request.



eprints@whiterose.ac.uk
<https://eprints.whiterose.ac.uk/>

1 An analysis of energy flow in a turbocharged diesel engine and potentials
2 of improving fuel economy and reducing exhaust emissions

3 Jianbing Gao^{a, b, c}, Haibo Chen^{c, *}, Guohong Tian^b, Chaochen Ma^{a, *}, Fei Zhu^a

4 ^a School of Mechanical Engineering, Beijing Institute of Technology, Beijing 100081,
5 China

6 ^b Department of Mechanical Engineering Sciences, University of Surrey, Guildford
7 GU27XH, UK

8 ^c Institute for Transport Studies, University of Leeds, Leeds LS2 9JT, UK

9

10 *Corresponding author: machaochen1900@163.com (Chaochen Ma)

11 H.Chen@its.leeds.ac.uk (Haibo Chen)

12

13 **Abstract:**

14 The impetus of the internal combustion engine developments is the reductions of the fuel
15 consumptions and exhaust emissions. Thermal management is an efficient method to decrease the
16 exhaust emissions and enhance fuel economy. In order to further optimize the thermal management
17 of internal combustion engines, a detailed analysis of the energy flow in each component of internal
18 combustion engines is indispensable. In this paper, the test bench of a heavy duty diesel engine was
19 established to obtain the target parameters. The energy distributions in each component of the diesel
20 engine, including compressor, intercooler, shaft power, turbine, coolant and exhaust, were
21 calculated using tested parameters. The lubricating oil consumption was also taken into
22 consideration. In addition, the potential influences of different turbochargers on the total thermal
23 efficiency were analyzed. The results showed that the thermal efficiency of the diesel engine was
24 more than 38% when the engine operated at 50%~100% engine load and 1000 rpm~1700 rpm
25 conditions. The energy loss by coolant was more than 50% of the total fuel energy consumption in
26 the low power output conditions. However, it was lower than 30% in high power output conditions,
27 and the thermal loss was more than 150 kW around rated power conditions. The maximum
28 proportion of the energy being consumed by turbine was ~10% of the fuel energy; additionally, the
29 exhaust energy distributions changed significantly after the turbine expansion. 1%~3% of the fuel
30 energy was recycled by the turbocharger, then, flowed into the cylinders. The energy loss through
31 the intercooler accounted for ~6% of the fuel energy. Significant reductions of exhaust emissions
32 and fuel consumptions can be achieved by optimizing the coolant and lubricating oil thermal
33 conditions. Turbochargers presented a huge effect on exhaust temperature distributions at high
34 power output conditions, and the total thermal efficiency changed significantly if all kinds of energy
35 recovery approaches were applied.

36

37 **Keywords:** diesel engines; energy distributions; thermal management; fuel economy; exhaust
38 emissions

39

40 **1. Introduction**

41 As the main power sources of the vehicles, internal combustion engines have attracted much
42 attention. Internal combustion engine powered vehicles will dominate the vehicle productions in the
43 following years, although electric and hybrid vehicles have more and more shares in the vehicle

44 market. Nevertheless, internal combustion engines encounter the challenges of decreasing exhaust
45 emissions and meeting the 95 g/km CO₂ emission targets in 2020 [1, 2]. Much energy is wasted in
46 the engine operation process by friction, coolant, exhaust and intercooler etc [3-6]. The energy
47 percentages in gasoline engines are ~40%, ~30% and ~25% for exhaust, coolant and effective
48 power output, respectively, while the power output is ~35% for diesel engines. The energy loss is
49 mainly in the form of heat; also, the energy grades of the waste heat are different, which causes the
50 systems complicate to recycle the waste heat.

51 Compared with the coolant heat, exhaust heat is at a high energy grade level, which has high
52 potentials of increasing the combined thermal efficiency of the engine and energy recovery systems.
53 Advanced technologies were used to recover exhaust energy, such as the thermoelectric generators
54 [7, 8], organic Rankine cycle (ORC) [9-11], the six-stroke cycle internal combustion engines [12, 13]
55 and novel turbochargers [14-16]. As the most successful technology of exhaust energy recovery,
56 turbochargers were used to increase the mass flow rate of fresh air for achieving a high energy
57 power density [17]. In order to meet the requirements of variable engine operation conditions on the
58 turbine expansion ratio, waste gate, variable nozzle turbines and variable geometric turbines [18]
59 were used, which significantly increased energy recovery efficiency, especially at low speed
60 conditions. The energy recycling percentage was closely related to turbine and compressor working
61 conditions, which made it important to excellently match the turbocharger with the engine.
62 Although turbocharger can effectively make use of exhaust energy, most of the exhaust energy
63 flowed into the atmosphere in the status of heat.

64 The researches about the exhaust and coolant thermal energy recovery are mainly focused on ORC
65 technology, which has the advantages of low requirements for energy grade level. Hou et al [19]
66 combined free piston expander-linear generator and ORC to recycle exhaust thermal energy. This
67 device was characterized with a small volume and a high power density, which made a huge step of
68 applying ORC to passenger vehicles. What's more, the maximum energy conversion efficiency
69 could reach 73.33% [20]. A dual-loop ORC system [21] was applied to achieve a higher energy
70 recycle efficiency. The net power output of a dual-loop ORC system reached 115.1 kW, which led
71 to a 11.6% increase of the engine power output. Compared with the exhaust heat, coolant heat was
72 at a low energy grade level, but the same order of magnitude in waste heat quantity. In order to
73 effectively recycle the coolant heat, CO₂-based transcritical Rankine cycle (CTRC) was researched
74 [22]. Boretti [23] used the ORC system to recycle the coolant heat of a 1.8 L naturally aspirated

75 gasoline engine, which was the power of a hybrid vehicle. Coolant ORC system could enhance the
76 fuel economy by averaged 1.7%, with a maximum value of 2.8%, which was lower than half of the
77 exhaust ORC system. In order to enhance the ORC system efficiency, the coolant was used to
78 pre-heat the working fluid of ORC system, as researched by Shu et al [24] who introduced an
79 improved CTRC system containing a pre-heater (namely, the intercooler in diesel engines) and a
80 regenerator (PR-CTRC). The net power output was 9.0 kW for a 43.8 kW engine, whose power
81 output increased by ~50% compared with the CTRC system. However, it had great challenges for
82 the ORC systems to be applied to the vehicles, which was partly caused by the huge size of the
83 systems and variable working conditions of internal combustion engines in the real driving
84 conditions. The dynamic engine operation conditions led to the working point variations of the
85 ORC components. Zhao et al [25] investigated the control strategy of the engine and ORC
86 combined system, where the optimal rotation speed of the fluid pump changed with engine
87 conditions. Variable-speed working fluid pumps could significantly increase the energy recover
88 efficiency of the ORC system. Jiménez-Arreola et al [26] analyzed the dynamic behaviors of the
89 heat exchanger used in the ORC system, where the louver fin multi-port flat tube evaporators had a
90 shorter response time compared with fin and tube evaporators, but penalty of high pressure drops of
91 exhaust and working fluid.

92 In most cases, coolant flow rate was higher than demanded values, which led to a lower engine
93 thermal efficiency and more exhaust emissions [27]. It was caused by the fact that the coolant flow
94 rate was proportional to the engine speed for conventional coolant pumps. So that the coolant and
95 lubricating oil were over-cooled for ~95% operation time [28]. In addition, the precisions of coolant
96 and lubricating oil temperature control were poor. Lower coolant and lubricating oil temperatures
97 meant poorer in-cylinder combustion, more serious cylinder quenching effect and higher friction
98 loss. Reference [29] demonstrated that 2%~5% fuel consumption drop, 10% HC and 20% CO
99 emission reductions were obtained when electric coolant pump was used to enhance the coolant
100 temperature from 90 °C to 110 °C. In reference [30], exhaust heat was stored in a heat storage
101 material, then, the heat was used to enhance the coolant and lubricating oil thermal condition when
102 necessary. This method effectively recycled parts of exhaust heat, also, decreased exhaust emissions
103 and friction loss. CO and HC emission reductions were 64% and 15%, respectively.

104 In order to recycle the energy of coolant, exhaust and intercooler with high efficiency, further, to
105 improve the fuel economy and decrease exhaust emissions, the energy flow in each component of

106 the internal combustion engine should be analyzed individually. Based on the energy flow, the
107 potentials of fuel economy improvement and emission reductions could be further analyzed. Luo
108 and Sun [31] researched the effect of the engine operation parameters on the energy flow in a
109 turbocharged hydrogen engine. Power output, coolant heat, lubricating oil heat, intercooler heat,
110 exhaust energy and missing energy were investigated. Rakopoulos and Giakoumis [32] used the
111 second-law to analyze the energy balance of a internal combustion engines, also, indicated that
112 turbocharger was an excellent second-law process to increase the engine power density.
113 Turbocharger system coupled the intake air and exhaust systems, which significantly influenced the
114 energy flow in diesel engines.

115 To authors' knowledge, a majority of the references [33-35] about the energy flow in internal
116 combustion engines united the turbocharger and engine. Literatures are limited to date about the
117 individual analysis of the energy flow in the engine and turbocharger. Also, the recycled energy by
118 turbocharger decreased greatly due to the heat loss through the intercooler. However, the researches
119 about the recycled energy flowing into the cylinders are few to refer. In addition, the heat
120 distributions of the intercooler were seldom investigated. The lubricating oil consumption during
121 engine operations was also neglected in many researches.

122 In this paper, the engine test bench was set up. Energy flow in the combustion process was
123 calculated based on the experimental data, with lubricating oil consumption being taken into
124 consideration to analyze the energy flow with a high precision. Different from previous studies, the
125 energy distributions in the engine and turbocharger were analyzed separately, which laid the
126 foundations of enhancing energy recovery efficiency. The recycled energy by turbocharger after the
127 intake air going through the intercooler was obtained. Then, the potentials of reducing exhaust
128 emissions and fuel consumptions were estimated. Further, the effect of different turbochargers on
129 the total thermal efficiency was investigated. The test bench refers to operative conditions ranging
130 between 20% and 100% of the load and between 800rpm and 2100 rpm.

131

132 **2. Experimental section**

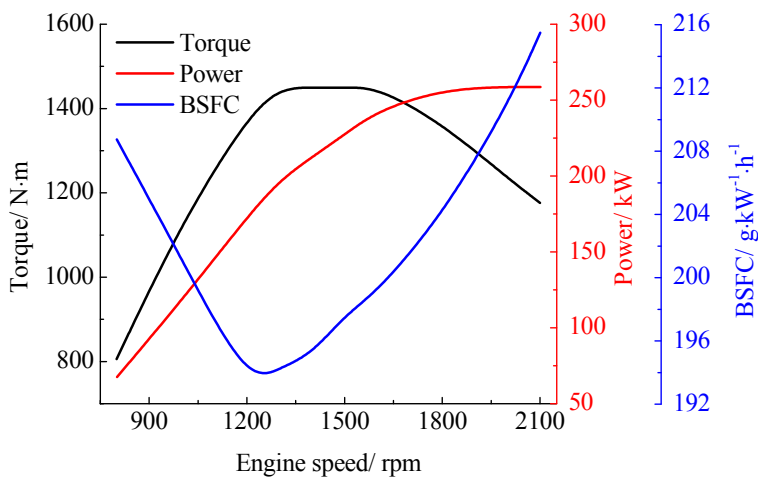
133 The demonstrator used in this study was a turbocharged heavy duty diesel engine; the specifications
134 of the diesel engine are shown in Table 1. Figure 1 shows the performances of the diesel engine at
135 full load conditions. The engine speed corresponding to the minimum brake specific fuel
136 consumption (BSFC) was ~1250 r/min, and BSFC increased dramatically when the engine speed

137 was deviated from that value.

138 Table 1 Specifications of the diesel engine

Items	Content
Engine type	In-line six cylinders, four-stroke
Max power/ kW	258
Max torque/ N·m	1450
Displacement/ L	8.6
Cylinder stroke/ mm	112
Cylinder bore/ mm	145
Compression ratio	17.5
Intake type	Turbocharged intercooler
Valve number per cylinder	4

139



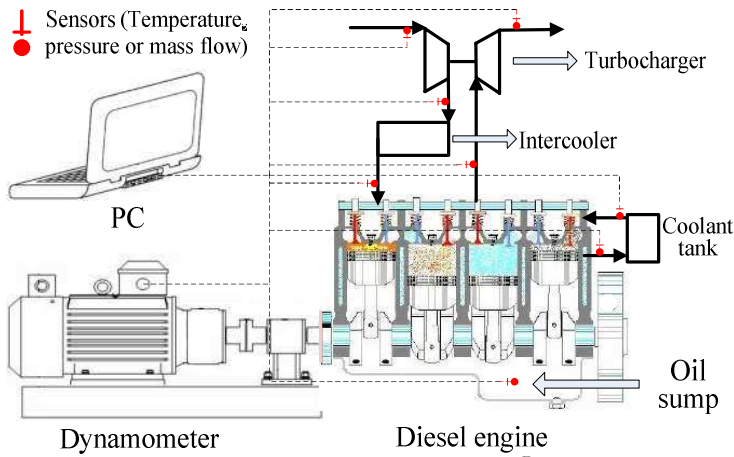
140

141 Figure 1 Performances of the diesel engine at full load conditions

142

143 Figure 2 shows the experimental system layout. The diesel engine was coupled with a dynamometer.
144 Temperatures and pressures were tested at the target points, such as compressor inlet and outlet,
145 turbine inlet and out let, intercooler outlet, coolant channel inlet and outlet, and oil sump. Coolant,
146 air flow rates and fuel consumption rate were also measured in the experiment. The temperature,
147 pressure and fluid flow rate were collected using a computer. The atmospheric temperature and
148 pressure were 20 °C and 1.0 bar, respectively. The engine operated for no less than 20 minutes to
149 ensure the engine fully warmed up after it started. It should be guaranteed that the coolant and oil
150 temperatures were stabilized when the data (temperature, pressure and fluid flow rate) was collected.

151 Instability of coolant and oil temperature could cause significant fluctuations of heat transfer,
152 friction loss and engine power output, which would influence the energy distributions in the diesel
153 engine. The lubricating oil consumption was considered as 0.2% of fuel consumption, which met
154 the standard of the engine manufacturers.

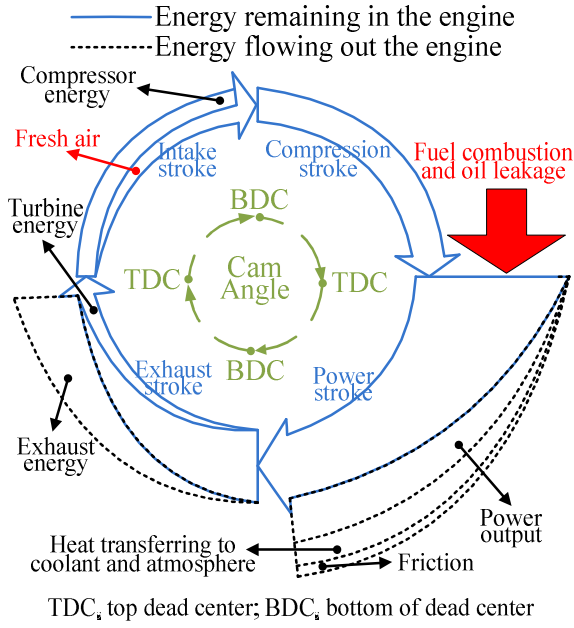


155
156 Figure 2 Layout of the experimental system

157

158 3. Energy distribution calculations

159 The temperature, pressure and mass flow rate collected in Section 2 were used to calculate the
160 energy distributions of each component in the whole combustion process. A control volume was
161 assumed around the engine to analysis the energy balance. Intercooler and turbocharger were
162 contained in the control volume, rather than the after-treatments. Fresh air, fuel and lubricating oil
163 were injected into the control volume; meanwhile, heat, torque and exhaust flowed out of the
164 control volume. The energy flow in a turbocharged diesel engine is shown in Figure 3, and the
165 exhaust gas recirculation (EGR) was neglected in the figure. Some process was considered as ideal
166 conditions, for example, the fuel injection and combustion was momentarily completed at the top
167 dead center (TDC), as shown in Figure 3. In the process of intake and compression strokes, the heat
168 transferring into the atmosphere was neglected due to its small value. Different from the naturally
169 aspired engine, parts of exhaust energy were recycled for the turbocharged engine, which
170 complicated the energy flow due to the turbocharger coupling the intake air and exhaust systems.



Assumptions:

1. The EGR was neglected.
2. The heat loss in the intake and compression strokes was neglected.
3. The fuel and lubricating oil were added into the system momentarily.
4. Lubricating oil consumption was considered as 0.2% of the fuel consumption.
5. The exhaust energy included the thermal energy and the chemical energy.

172 Figure 3 Energy flow in the turbocharged diesel engine

173 Based on the first law of thermodynamics, the energy balance in the diesel engine is shown in
 174 Equation 1,

$$175 \quad \dot{Q}_f + \dot{Q}_a + \dot{Q}_{cc} = \dot{Q}_p + \dot{Q}_e + \dot{Q}_c + \dot{Q}_i + \dot{Q}_u + \dot{Q}_T \quad (1)$$

176 Where, \dot{Q}_f , chemical energy of the fuel (including diesel fuel and leaked lubricating oil); \dot{Q}_a ,
 177 energy of the fresh air; \dot{Q}_{cc} , energy consumption by the compressor; \dot{Q}_p , power output through
 178 shaft; \dot{Q}_e , exhaust energy flow out of the system; \dot{Q}_c , heat transferring to the coolant; \dot{Q}_i , heat
 179 transferring to the intercooler; \dot{Q}_T , energy generated by the turbine; \dot{Q}_u , unaccounted heat loss.

180 Unaccounted heat loss refers to the heat transferring to the atmosphere by the convection and
 181 radiation transfer. In the process of the engine operations, the friction loss accounts for a large
 182 proportion of the energy loss. This part of energy is lost in the status of heat. In order to decrease the
 183 piston wear and friction loss, lubricating oil film is existed in the gaps of cylinder liners and pistons,
 184 which unavoidably leads to the combustion of lubricating oil in cylinders. The lubricating oil
 185 leakage is considered to be 0.2% of the fuel consumption [36, 37]. The chemical energy supplied by
 186 the fuel and lubricating oil is shown in Equation 2,

$$187 \quad \dot{Q}_f = Q_{f_LHV} \cdot \dot{m}_f + Q_{o_LVH} \cdot \dot{m}_o \quad (2)$$

188 Where, Q_{f_LHV} and Q_{o_LVH} are the low heating values of the fuel (46.04 MJ/kg) and lubricating
 189 oil (36.00 MJ/kg) respectively; \dot{m}_f and \dot{m}_o are fuel and lubricating oil consumption rates (kg/s),

190 respectively.

191 The energy of the fresh air is calculated using Equation 3,

$$192 \quad \dot{Q}_a = \Delta h_a \cdot \dot{m}_a \quad (3)$$

193 Where, Δh_a is the enthalpy difference of the fresh air from the standard status (kJ/kg); \dot{m}_a is the
194 fresh air flow rate (kg/s). The enthalpy is referred from the data of National Institute of Standards
195 and Technology (NIST), which takes the water and CO₂ in the air into consideration.

196 The exhaust energy is as following,

$$197 \quad \dot{Q}_e = \Delta h_e \cdot \dot{m}_e \quad (4)$$

198 Where, Δh_e is the enthalpy difference of the exhaust from the standard status (kJ/kg), the value is
199 obtained from NIST database; \dot{m}_e is the exhaust flow rate (kg/s).

200 Energy transferring to the coolant is calculated using Equation 5. Because the heat transferring to
201 the lubricating oil is low, it is classified into the unaccounted heat loss \dot{Q}_u . Also, most of the heat
202 of lubricating oil is transferred to the coolant.

$$203 \quad \dot{Q}_c = \dot{m}_c \cdot C_c \cdot \Delta T_c \quad (5)$$

204 Where, \dot{m}_c is the coolant flow rate (kg/s); C_c is the heat capacity of the coolant (4.2 kJ·kg⁻¹·K⁻¹);
205 ΔT_c is the temperature difference of the coolant that flows into and out of the engine block.

206 For a turbocharged diesel engine, the air temperature of the compressor outlet is high, which drops
207 the air density significantly. Intercooler can effectively decrease the fresh air temperature. The heat
208 transferring to the intercooler is calculated using Equation 6,

$$209 \quad \dot{Q}_i = \dot{m}_a \cdot \Delta h_i \quad (6)$$

210 Where, \dot{m}_a is the fresh air flow rate (kg/s); Δh_i is enthalpy difference of fresh air from the
211 standard status (kJ/kg). The value is based on NIST database.

212 Turbocharger couples exhaust and intake air systems, which makes energy flow more complicated.
213 In addition, the efficiency of the compressor and turbine dominates the exhaust energy utilization
214 efficiency. Equation 7 shows the efficiency calculation of the compressor,

$$215 \quad \eta_c = (h_{2s} - h_1)/(h_2 - h_1) = (T_{2s} - T_1)/(T_2 - T_1) \quad (7)$$

216 Where, h_1 , h_2 and h_{2s} are air enthalpy of compressor inlet (kJ/kg), air enthalpy of compressor

217 outlet (kJ/kg), and air enthalpy of compressor outlet (kJ/kg) if isentropic compression, respectively.
 218 T_1 , T_2 and T_{2s} are compressor inlet temperature (K), compressor outlet temperature (K), and
 219 compressor outlet temperature (K) if isentropic compression, respectively. Equation 8 shows the
 220 T_{2s} calculation,

$$221 \quad T_{2s} = (P_2 / P_1)^{\frac{\kappa_a - 1}{\kappa_a}} T_1 \quad (8)$$

222 Where, P_1 , P_2 , T_1 and κ_a are compressor inlet pressure (Pa), compressor outlet pressure (Pa),
 223 compressor inlet temperature (K), and specific heat ratio of air (1.4), respectively.

224 Equation 9 shows the calculation of compressor power consumption,

$$225 \quad P_c = (h_2 - h_1) \cdot \dot{m}_a \quad (9)$$

226 The efficiency calculation of the turbine is shown in Equation 10,

$$227 \quad \eta_T = (h_3 - h_4) / (h_3 - h_{ST}) = \Delta h_T / \Delta h_{ST} \quad (10)$$

228 Where, h_3 , h_4 and h_{ST} are exhaust enthalpy of turbine inlet (kJ/kg), exhaust enthalpy of turbine
 229 outlet (kJ/kg), and exhaust enthalpy of turbine outlet (kJ/kg) if isentropic expansion respectively.

230 The calculation of h_{ST} is shown in Equation 11,

$$231 \quad \Delta h_{ST} = \frac{\kappa_3}{\kappa_3 - 1} R T_3 \left[1 - \left(\frac{1}{\pi_T} \right)^{\frac{\kappa_3 - 1}{\kappa_3}} \right] \quad (11)$$

232 Where, κ_3 , T_3 , R and π_T are exhaust specific heat ratio of at turbine inlet, exhaust temperature of
 233 turbine inlet (K), gas constant ($8.314 \text{ J} \cdot \text{mol}^{-1} \cdot \text{K}^{-1}$), and expansion ratio of turbine respectively.

234 Equation 12 shows the power consumed by turbine,

$$235 \quad P_T = (h_3 - h_{ST}) \cdot (\dot{m}_a + \dot{m}_f + \dot{m}_o) / (\eta_{mT} \cdot \eta_{mC} \cdot \eta_{sh}) \quad (12)$$

236 Where, η_{mT} , η_{mC} and η_{sh} are mechanical efficiency of turbine, compressor and shaft,
 237 respectively.

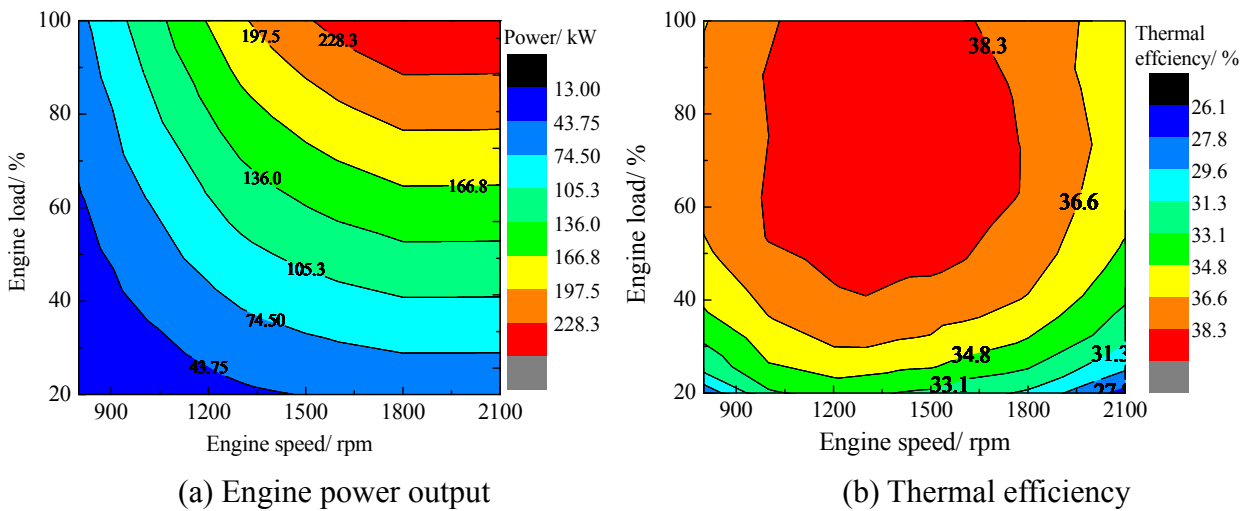
238

239 **4. Results and discussion**

240 **4.1 Engine power output distributions**

241 The target engine is used for a heavy duty truck, the engine power output and thermal efficiency at
 242 different engine operation conditions are shown in Figure 4. The thermal efficiency of the diesel

243 engine was higher than 26% at all the researched operation conditions, and it was higher than 38%
 244 only when engine load was higher than 40%. However, internal combustion engines regularly
 245 operate at low speed and load conditions when vehicles run in urban driving cycles. Much energy is
 246 lost in the status of heat, mainly by the coolant and exhaust. There are huge potentials for the diesel
 247 engine to improve the energy utilization efficiency by thermal management, such as, recycling the
 248 heat of the coolant, intercooler and exhaust, and optimal coolant and lubricating oil temperature.
 249 Analysis of the energy flow in the diesel engine operation process provides the foundations of
 250 thermal management. Gharehghani et al. [34] investigated the energy flow of a turbocharged spark
 251 ignition engine, which considered the intercooler heat loss and leaked lubricating oil combustion,
 252 also, calculated the unaccounted heat loss. The unaccounted heat loss was mainly caused by the
 253 convection and radiation transfer. However, the heat loss by the coolant and intercooler was
 254 analyzed jointly although different energy grade levels. The energy distribution analysis of turbine
 255 and compressor were neglected, which had a huge effect on the energy flow in internal combustion
 256 engines.

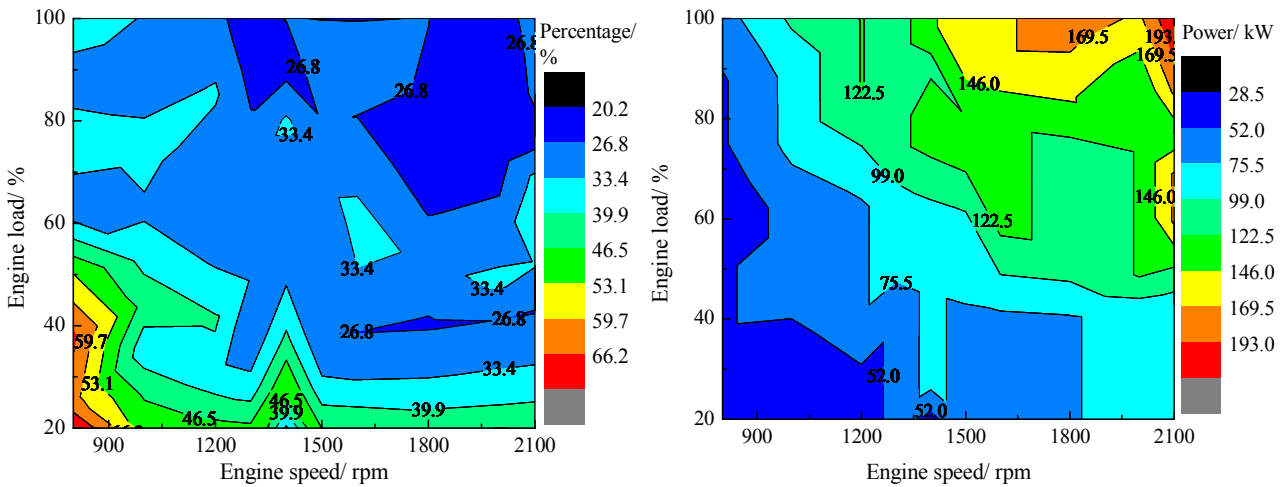


259 Figure 4 Engine power output and thermal efficiency distributions

260 4.2 Energy distributions of coolant system

261 In order to prevent the engine block overheating, cooling system is necessary to keep the engine
 262 block at an appropriate temperature level. Large percentage of heat is transferred from the coolant
 263 to the atmosphere; also, it greatly depended on the engine operation conditions. Due to the
 264 lubricating oil being cooled by the coolant, the coolant accounted for ~96% of the total cooling heat.
 265 As indicated by Jung et al. [38] that the heat loss caused by the coolant accounted for 70.1% of the
 266 total cooling loss, and it was 16.1% for the lubricating oil, in addition, 4.8% heat loss was caused by
 267 convection and radiation transfer. Figure 5 shows the coolant energy loss distributions at different

268 engine operation conditions. The percentage of the energy calculated in this paper referred to the
 269 percentage of target energy in the total fuel chemical energy, except where noted. The share of the
 270 coolant heat loss was more than 50% for the engine operating at low power output conditions, and it
 271 was ~30% for high load and speed conditions. The maximum energy loss was ~193 kW when
 272 engine operated around the rated power condition. High coolant heat loss led to a low brake thermal
 273 efficiency that such large amounts of energy should be effectively recycled. The energy recycling
 274 devices should consider the high power output conditions, because large quantities of heat were lost
 275 although engine seldom operated around the rated power conditions. The design point of the
 276 traditional cooling system was the maximum heat loss condition, meanwhile, the coolant flow rate
 277 was proportional to the engine speed for the conventional coolant pump, which led to the redundant
 278 heat loss at part load conditions [39]. More heat loss partly caused lower thermal efficiency, also,
 279 excess coolant flow rate led to more energy consumption of coolant pump [28, 29, 40]. As can be
 280 seen, some unexpected contour lines existed (e.g. around 60% load and 1650 rpm), which was
 281 resulted from data interpolation error.



282 (a) Energy percentage

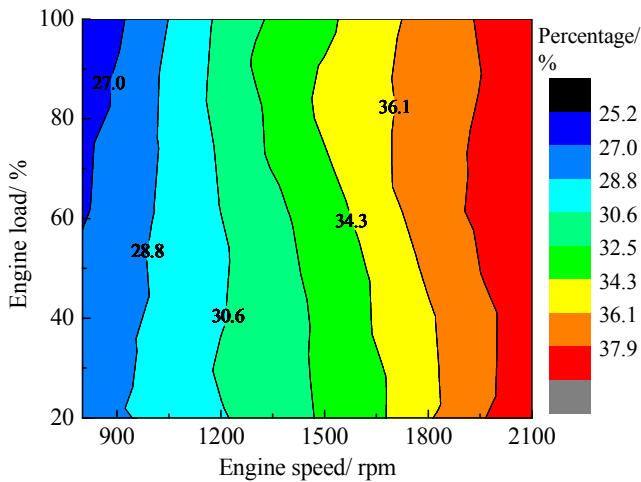
283 (b) Energy quantity

284 Figure 5 Energy loss distributions by coolant

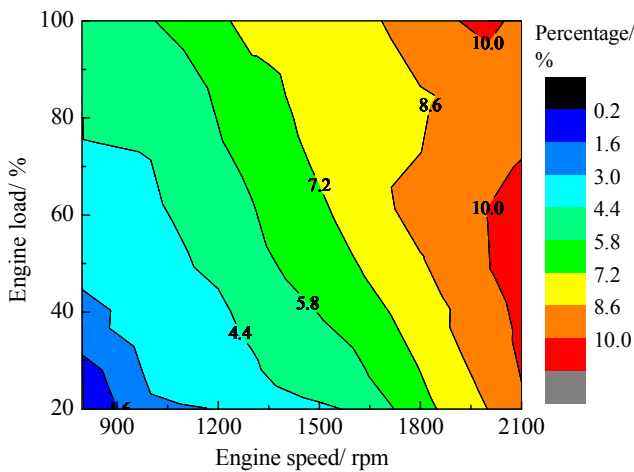
285 **4.3 Energy distributions of turbocharger system**

286 Coolant and exhaust energy dominate the energy loss of the diesel engines, the exhaust energy
 287 distributions before turbine are shown in Figure 6. The energy loss percentage increased with the
 288 engine speed; in addition, the engine load presented a smaller effect on the energy distributions than
 289 the engine speed. The energy percentage ranged from ~25% to ~38%, which was in the same level
 290 with the engine brake thermal efficiency. High exhaust temperature and flow rate caused a huge
 291 exhaust energy percentage at high speed conditions, which partly caused the low thermal efficiency.

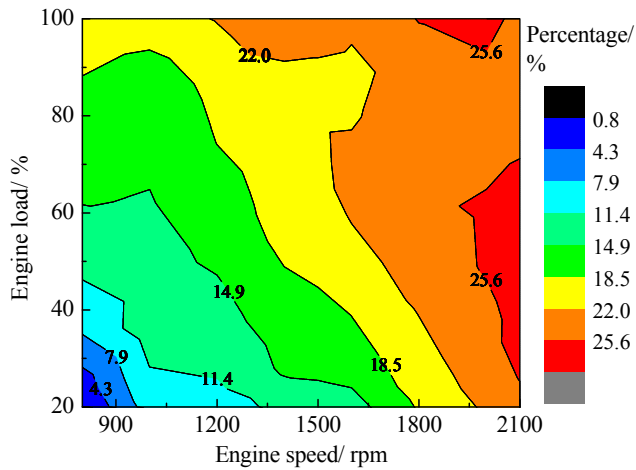
292 Turbocharger as an effective method to recycle the exhaust energy was widely applied to the
 293 internal combustion engines [41-43]. Figure 7 shows the distributions of the energy consumed by the
 294 turbine. Being enslaved to the maximum cylinder pressure and thermal load, the waste-gate was
 295 in a large opening at high power output conditions, which caused less energy to be recycled by
 296 turbine. A noteworthy phenomenon was observed by comparing Figures 6 and 7 that the exhaust
 297 energy percentage was the lowest (~27%) around 800 rpm and 100% load conditions, where the
 298 percentage of the energy consumed by the turbine was at a general level (~5%). Higher brake
 299 thermal efficiency around this point (800 rpm and 100% load) partly led to the low percentage of
 300 exhaust energy before turbine, meanwhile, high exhaust temperature and pressure partly explained
 301 the high recycle efficiency (recycled energy over exhaust energy) of turbine (Figure 8).



302
 303 Figure 6 Exhaust energy distributions before turbine



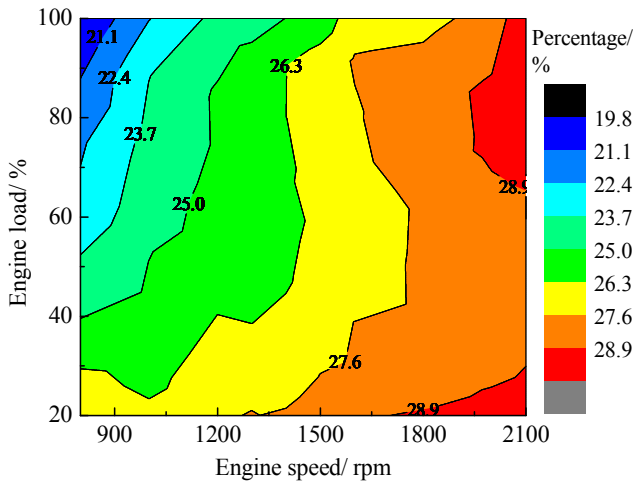
304
 305 Figure 7 Distributions of energy consumed by turbine



306

307 Figure 8 Distributions of energy recycled percentage

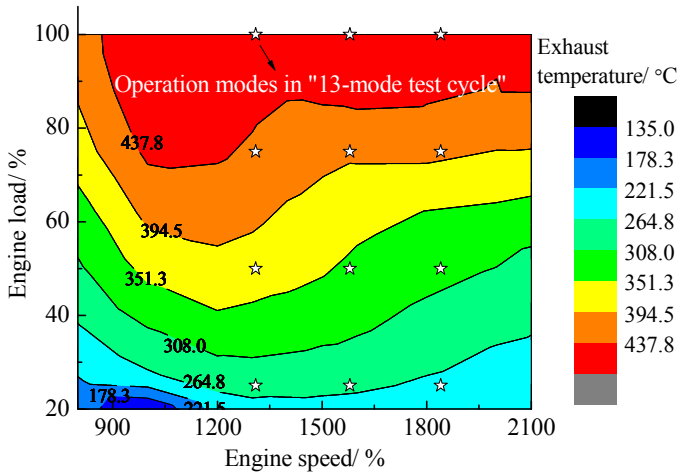
308 The exhaust energy percentage after turbine was more than 25% at majority of the engine operation
 309 conditions, as shown in Figure 9. The exhaust energy was ~30% for the high speed conditions. The
 310 exhaust energy was further recycled using a two-stage turbocharger which contributed to the engine
 311 downsize [44]. In reference [45], a two-stage turbocharger was used to recover the engine power at
 312 plateau or to obtain higher power density, with the results of more complicated energy flow in the
 313 system. Exhaust temperature decreased greatly after passing the turbine, which lowered the energy
 314 grade, however, the heat quantity was still ~25% in the fuel chemical energy. ORC systems [46-48]
 315 and CO₂ transcritical waste heat recovery systems [49, 50] were used to recycle the exhaust energy
 316 after turbine. After passing through the evaporator of the single stage Rankine cycle, the exhaust
 317 temperature was still high despite of a lower grade level of the heat energy. In order to further
 318 recycle the exhaust energy, the double stage and triple stage Rankine cycle were used [51], a
 319 maximum power of 517.27 kW was recycled from a 2928 kW diesel engine, whose exhaust
 320 temperature was ~470 °C. Although complicated equipments for multiple stage Rankine cycle, ~50%
 321 of the exhaust energy could be recycled. Estimated from the reference [51], a maximum recycled
 322 power of 50 kW could be achieved using the system for the diesel engine in the paper. It should be
 323 noted that high energy recycling efficiency was obtained in many researches, where after-treatment
 324 systems were neglected that the after-treatment should be positioned before ORC system. High
 325 temperature was need to light-off catalysts, and much heat was lost through catalysts and pipes,
 326 which would decrease the energy recycling efficiency. Meantime, the oxidations of hydrocarbon
 327 and carbon monoxide released much heat, however, the hydrolysis of ammonium hydroxide was a
 328 endothermic reaction. The research about the effect of ORC system and after-treatment layout on
 329 the energy recycle efficiency should be further performed.



330

331 Figure 9 Exhaust energy distributions after turbine

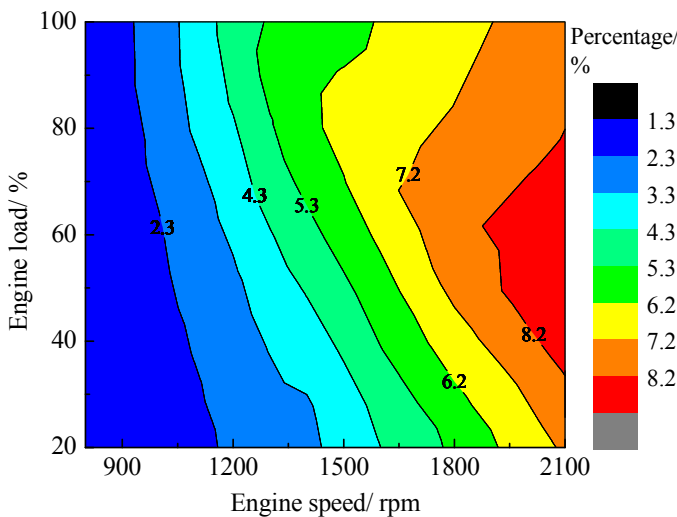
332 In order to meet the requirements of the stringent emission regulations, diesel oxidation catalyst
 333 (DOC) and selective catalytic reduction (SCR) are used to decrease the exhaust emissions. High
 334 temperature is needed to light-off the catalysts to achieve high catalytic efficiency. The exhaust
 335 energy could be used to heat the catalysts when catalysts were in the inefficiency conditions. Figure
 336 10 presents the exhaust temperature distributions after turbine, and 12 operation points in “13-mode
 337 test cycle”. As can be seen, the temperatures of 3 low load operation points were ~ 220 °C where
 338 DOC and SCR were fully light-off. As indicated in references [52-54], PM ignition temperature was
 339 more than 450 °C for non-catalytic DPF. Temperature was much low to achieve DPF regeneration
 340 at part load conditions, the phenomenon was more serious at cold start and warm up conditions.
 341 Thermal management was adopted to increase the exhaust temperature [55], such as delaying the
 342 start of combustion [56], burners [57], heat storage materials [30] and electrical heated catalysts
 343 [58]. Kauranen et al. [59] adopted a latent heat accumulator to storage exhaust thermal energy
 344 which could be used to fast light-off catalyst at cold start conditions. This device could replace the
 345 extra heater and eliminate the fuel penalty. Exhaust energy recycling should be combined with
 346 after-treatment systems to achieve the optimal energy efficiency under the conditions of meeting
 347 emission regulations.



348

349 Figure 10 Distributions of exhaust temperature after turbine

350 Turbocharger couples intake air and exhaust systems, which make the energy flow
 351 cross-correlations in turbine and compressor. Energy consumption percentage distributions of
 352 compressor are shown in Figure 11, and the efficiency distributions are presented in Figure S1.
 353 Compressor efficiency was higher than 65% for majority of the operation points. Energy
 354 consumption by compressor ranged from ~2% to ~8%, and the distributions were dramatically
 355 different from turbine. The energy consumed by compressor increased generally with engine power
 356 when the engine load and speed were low. Waste-gate of turbine was in a large opening when
 357 engine power output was huge, being restricted by the cylinder peak pressure and thermal load,
 358 which decreased the energy consumption percentage.



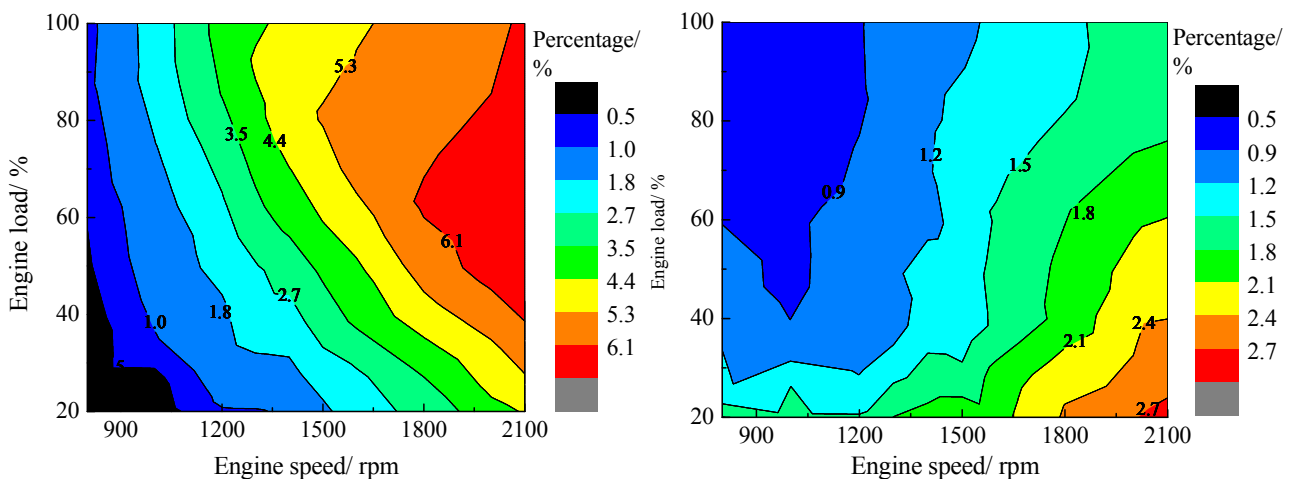
359

360 Figure 11 Energy consumption percentage distributions of the compressor

361 **4.4 Energy distributions of intercooler system**

362 In order to increase the intake air density, decrease engine thermal load and NO_x emissions,
 363 intercooler is necessary to decrease the intake air temperature. Much heat was transferred to the

364 atmosphere through intercooler, as shown in Figure 12(a). The air flow rate, inlet and outlet
 365 temperatures of intercooler are shown in Figure S2~S4, respectively. The maximum percentage of
 366 the heat loss was more than 6.1% of the total fuel chemical energy. Pressure ratio of compressor
 367 was small at low engine speed and load conditions, where the heat loss by the intercooler was
 368 smaller than other conditions. Figure 12(b) shows the distributions of recycled energy flowing into
 369 the cylinders. Only 1%~3% of the total fuel chemical energy flowed into the cylinders eventually to
 370 increase the intake air flow rate. High engine speed and low load conditions showed the hugest
 371 percentage. Due to its low temperature of compressor outlet, this made it hard to recycle this part of
 372 energy. Shu et al. [24] used a pre-heater (improved intercooler in the diesel engine) to recycle the
 373 heat of intercooler, using CO₂-based transcritical Rankine cycle. The working fluid passed the
 374 pre-heater firstly to absorb the heat of the intercooler, then, flowed to the evaporator to recycle the
 375 exhaust thermal energy. This method showed an excellent performance of recycling intercooler and
 376 exhaust energy.



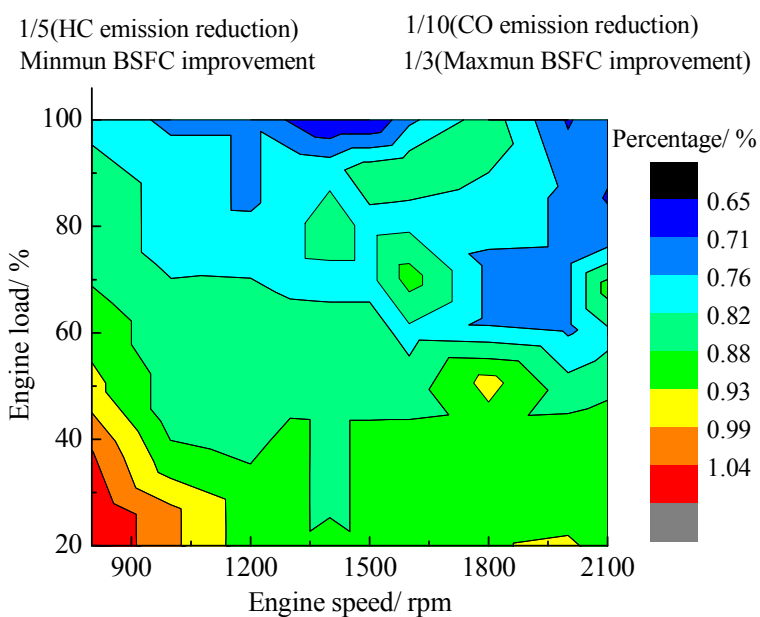
377
 378 (a) Distributions of energy transferred by intercooler (b) Recycled energy flowing into cylinders

379 Figure 12 Energy distributions of intercooler system

380 4.5 Potentials of decreasing emissions and BSFC by optimizing coolant and oil temperature

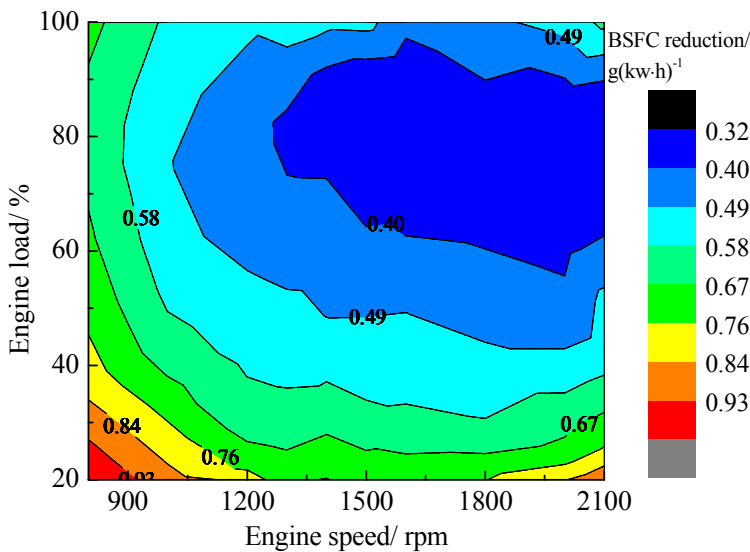
381 For the conventional internal combustion engines, coolant pumps were actuated directly using shaft
 382 that the coolant flow rate was proportional to engine speed [28]. In addition, the designs of the
 383 coolant pumps were based on the maximum heat transfer conditions, with the results of engines'
 384 overcooling at the other conditions. Also, waxy thermostats were insensitive to the engine coolant
 385 temperature, which made the coolant temperature control with a low precision. Allen et al. [60]
 386 showed that the coolant pump in conventional engines produced much more coolant flow rate than
 387 required value that the phenomenon reached up to 95% the total operation time. The temperature of

388 the coolant flowing out of the engine block is shown in Figure S5. Overcooling of the engine block
 389 caused poor cylinder combustion and serious cylinder quenching effect, with the results of high
 390 BSFC and exhaust emissions. References [61-63] adopted electric pump and electric thermostat to
 391 control the coolant temperature to ensure the excellent thermal status of coolant. As indicated by
 392 Chanfreau et al. [29], it reduced 2%~5% fuel consumption, 10% tailpipe HC and 20% CO
 393 emissions when the coolant temperature was increased from 90 °C to 110 °C. The potentials of
 394 BSFC and emission reductions are shown in Figure 12 The optimal temperature of the coolant
 395 flowing out of the engine block was considered as 90 °C in this paper. The coolant temperature
 396 optimization could be achieved by electric pump or heat storage approaches [55]. Low engine speed
 397 and load conditions showed the maximum performance improvement that the BSFC decreased by
 398 ~3%, and emission reduction was ~10% by increasing the coolant temperature to 90 °C. The
 399 operation conditions around the rated power showed the smallest BSFC and emission reductions.
 400 Higher coolant temperature meant less heat transferring to the coolant from the engine block, which
 401 contributed to enhanced thermal efficiency. Higher coolant temperature also contributed to the
 402 air/fuel mixture formation, which caused better in-cylinder combustion and less quenching effect. In
 403 addition, the coolant pump could be downsized to further decrease the coolant pump energy
 404 consumption. Less heat transferred to the coolant could also decrease the power consumption of fan.
 405 Also, some unexpected contour lines existed were observed, which was resulted from data
 406 interpolation error.



407
 408 Figure 13 Potentials of BSFC and emission reductions by optimizing coolant temperature
 409 Temperature of the lubricating oil was lower than the optimal value in one third of the trips [64],

410 and the maximum friction losses in the warm up process were 2.5 times higher than the optimal
 411 temperature conditions [65, 66]. Similar to the electric coolant pumps, electric oil pumps could be
 412 used to decrease the energy loss and emissions, also, the energy consumption of oil pumps. The
 413 optimal temperature was considered as 110 °C in this paper, the estimated BSFC reduction after
 414 enhancing lubricating oil temperature is shown in Figure 13. Temperature distributions of the
 415 lubricating oil in different engine operation conditions are shown in Figure S6. The potential of
 416 maximum BSFC reduction by using the electric oil pump was $\sim 1 \text{ g}/(\text{kW}\cdot\text{h})$, where the engine ran at
 417 low speed and load conditions. The least BSFC improvement was $\sim 0.4 \text{ g}/(\text{kW}\cdot\text{h})$, where the engine
 418 operated at high load and speed conditions, in which the in-cylinder temperature was much high.
 419 The potentials for the hybrid electric vehicles (HEVs) improvement is huger, because regular
 420 start-stop conditions are common, which makes the engine more frequently operate at low coolant
 421 and oil temperature conditions. Intelligent control of the coolant pump and oil pump is necessary to
 422 control the coolant and oil temperature with a high precision.



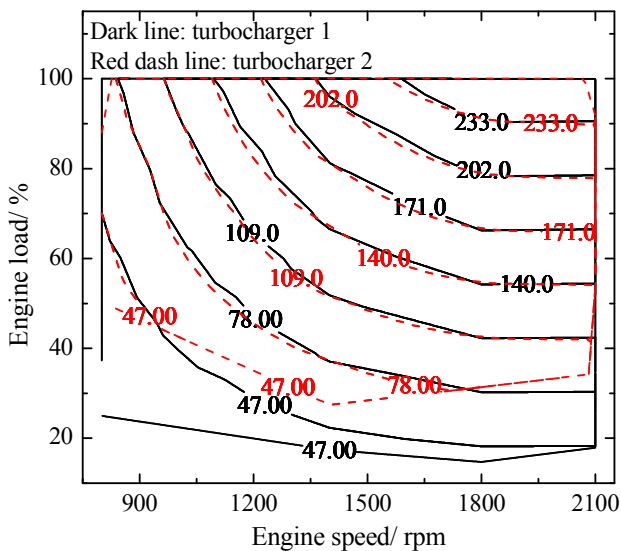
423
 424 Figure 14 Potentials of BSFC reduction by increasing oil temperature

425 4.6 The effect of different turbocharger systems

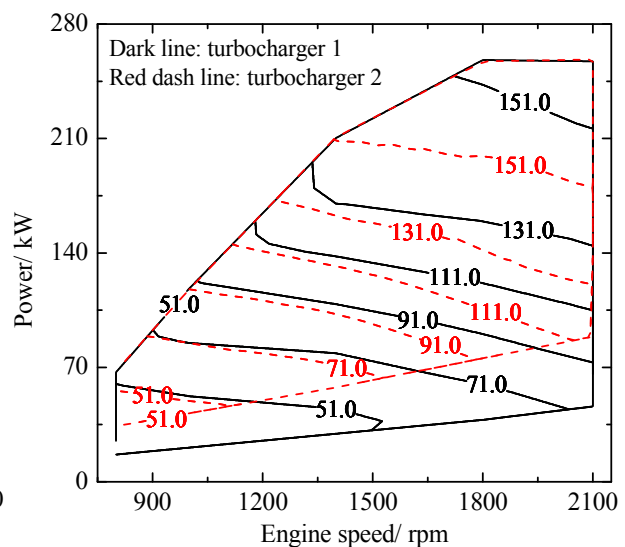
426 In the process of engine operations, turbochargers have a huge effect on the energy flow, resulting
 427 from the coupling of the intake and exhaust systems. Higher power output of the turbine contributes
 428 to higher intake air density; however, it causes higher engine backpressure. Abedin et al. [35]
 429 reviewed the effect of turbocharger on the energy balance. The BSFC of the internal combustion
 430 engine decreased by $\sim 5\%$, and with another $\sim 5\%$ improvement if the intercooler device was adopted.
 431 The heat loss by diesel exhaust decreased from $\sim 35\%$ to $\sim 30\%$ because of the turbocharger
 432 application, however, the coolant heat loss increased due to high thermal load caused by a higher

433 power density.

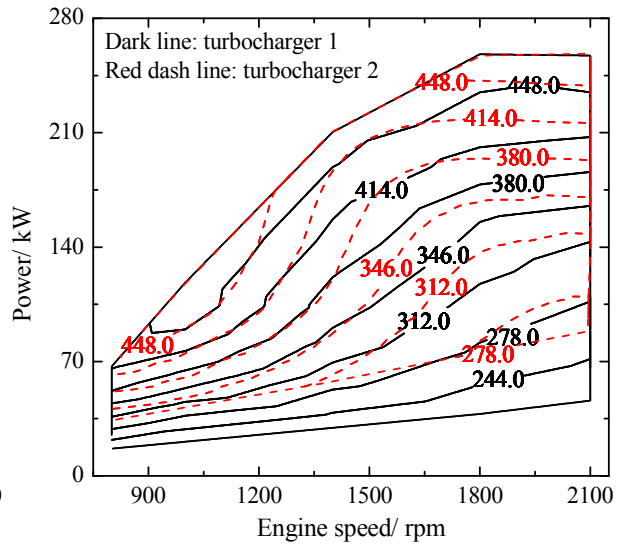
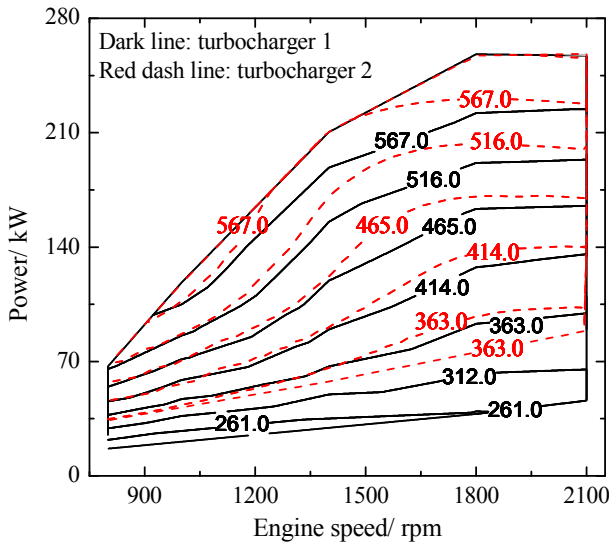
434 Figure 15 shows the effect of different turbochargers on the engine performance. In the above
435 research, the turbocharger 1 was used because only the power output and brake thermal efficiency
436 were considered when choosing the turbocharger. However, the situation may change if all kinds of
437 energy recovery approaches were conducted. As can be seen from Figure 15(a), the power output of
438 the diesel engine increased slightly at high engine speed and low load conditions after turbocharger
439 2 was applied; however, it decreased at low and medium engine speed and load conditions, where
440 the engine normally operated in real driving conditions. The outlet temperature of the compressor
441 increased after adopting turbocharger 2 at majority of the operation conditions. Also, the
442 temperature difference was huger at higher power output conditions. Higher compressor outlet
443 temperature was caused by higher compression ratio, which also caused more heat loss by
444 intercooler. The inlet and outlet temperatures of the turbine were lower for turbocharger 2 compared
445 with turbocharger 1. It presented a small influence on turbine inlet and outlet temperatures at low
446 power output conditions. The temperature differences of turbine outlet would cause different energy
447 recovery efficiency, such as the two-stage turbochargers, ORC systems. In addition, the outlet
448 temperature of turbine was closely related to after-treatment performance. In the enhanced
449 after-treatment systems, effective heating measures were needed to fast light-off catalyst [66, 67].
450 The detailed investigations of the effect of different turbochargers on the energy flow in diesel
451 engines will be further conducted.



452 (a) Engine power output



453 (b) Temperature of compressor outlet



(c) Temperature of turbine inlet

(d) Temperature of turbine outlet

Figure 15 Effect of turbochargers on the energy distributions

5. Conclusion

In order to decrease the diesel exhaust emissions and fuel consumptions using thermal management methods, energy flows in a turbocharged diesel engine were analyzed, including the energy distributions of the engine power output, coolant, lubricating oil, turbine, compressor and intercooler systems. The main conclusions are as the following:

- (1) The brake thermal efficiency of the diesel engine was more than 33% at majority of the engine operation conditions, with the maximum value being more than 38%.
- (2) The coolant energy ranged from 30 kW~190 kW, and the minimum percentage was more than 26% of the total fuel chemical energy, also, the maximum value was ~66%. The potentials of coolant energy recycling were promising, although the energy grade level was low, if excellent thermal management methods were used. Exhaust energy consumed by the turbine was in the range of 1.6%~10.4%, which changed the exhaust energy distributions; meanwhile, the changes were significant when the engine loads were smaller than 50%.
- (3) The tendency of the contour lines of energy distributions were similar for compressor and intercooler, resulting from the fact that higher energy consumption by compressor would led to higher heat loss by intercooler. The recycled exhaust energy eventually flowing into the engine cylinders was in the range of 1%~3% due to much heat loss in the intercooler.
- (4) The estimated of BSFC improvement was 0.65%~1.95% by optimizing coolant temperature, also, it was 0.31 g/(kW·h)~0.93 g/(kW·h) for lubricating oil. In addition, the HC and CO emissions

477 could be reduced by 3.25%~5.2% and 6.5%~10.4%, respectively when the coolant temperature was
478 kept at 90 °C using electric coolant pump and electric thermostat.

479

480 It should be noted that the choosing of the turbocharger for a diesel engine is basically based on the
481 power output and brake thermal efficiency. The conditions will change if the energy recycling and
482 thermal management approaches (e.g. ORC) are used. The effect of different turbochargers on the
483 energy flow in the diesel engine after the application of energy recycling approaches should be
484 further analyzed. It may lead to the changes of the matching criteria for turbocharger with the
485 engine.

486

487 **Acknowledgement**

488 The research described in this paper was supported in part by the EU-funded project optiTruck
489 (grant agreement No 713788) which has the ultimate aim to develop and test a prototype ‘global
490 optimizer’, capable of achieving a fuel reduction of at least 20% for 40 tonne trucks while still
491 meeting relevant Euro VI emission standards.

492

493 **Support information**

494 This section provides the information about the efficiency distributions of compressor, air flow rate
495 distributions, temperature distributions of intercooler inlet, temperature distributions of intercooler
496 outlet, temperature distributions of coolant flowing out of engine block and Temperature
497 distributions of lubricating oil.

498

499 **Reference**

500 [1] T.V. Johnson. Review of vehicular emissions trends. SAE International Journal of Engines. 8
501 (2015) 1152-67.

502 [2] V. Novelli, P. Geatti, L. Ceccon, L. Toscani. Low environmental impact of alternatively supplied
503 cars. Results of an investigation carried out in the north-east of Italy. Environmental Engineering &
504 Management Journal (EEMJ). 16 (2017).

505 [3] J.R. Blantin, J. Ausserer, M.D. Polanka, P.J. Litke, J.A. Baranski. Power Loss Pathways and
506 Energy Balance of a Small Four-Stroke Internal Combustion Engine. 55th AIAA Aerospace
507 Sciences Meeting2017. p. 0389.

- 508 [4] C. Sprouse III, C. Depcik. Review of organic Rankine cycles for internal combustion engine
509 exhaust waste heat recovery. *Appl Therm Eng.* 51 (2013) 711-22.
- 510 [5] M. He, X. Zhang, K. Zeng, K. Gao. A combined thermodynamic cycle used for waste heat
511 recovery of internal combustion engine. *Energy.* 36 (2011) 6821-9.
- 512 [6] S. Quoilin, R. Aumann, A. Grill, A. Schuster, V. Lemort, H. Spliethoff. Dynamic modeling and
513 optimal control strategy of waste heat recovery Organic Rankine Cycles. *ApEn.* 88 (2011) 2183-90.
- 514 [7] T.Y. Kim, A.A. Negash, G. Cho. Waste heat recovery of a diesel engine using a thermoelectric
515 generator equipped with customized thermoelectric modules. *Energy Convers Manage.* 124 (2016)
516 280-6.
- 517 [8] T.Y. Kim, S. Lee, J. Lee. Fabrication of thermoelectric modules and heat transfer analysis on
518 internal plate fin structures of a thermoelectric generator. *Energy Convers Manage.* 124 (2016)
519 470-9.
- 520 [9] S. Lecompte, H. Huisseune, M. van den Broek, S. De Schampheleire, M. De Paepe. Part load
521 based thermo-economic optimization of the Organic Rankine Cycle (ORC) applied to a combined
522 heat and power (CHP) system. *ApEn.* 111 (2013) 871-81.
- 523 [10] M. Preißinger, J.A. Schwöbel, A. Klamt, D. Brüggemann. Multi-criteria evaluation of several
524 million working fluids for waste heat recovery by means of Organic Rankine Cycle in passenger
525 cars and heavy-duty trucks. *ApEn.* 206 (2017) 887-99.
- 526 [11] F. Alshammari, A. Pesyridis, A. Karvountzis-Kontakiotis, B. Franchetti, Y. Pasmazoglou.
527 Experimental study of a small scale organic Rankine cycle waste heat recovery system for a heavy
528 duty diesel engine with focus on the radial inflow turbine expander performance. *ApEn.* 215 (2018)
529 543-55.
- 530 [12] J.C. Conklin, J.P. Szybist. A highly efficient six-stroke internal combustion engine cycle with
531 water injection for in-cylinder exhaust heat recovery. *Energy.* 35 (2010) 1658-64.
- 532 [13] E. Arabaci, Y. İçingür, H. Solmaz, A. Uyumaz, E. Yilmaz. Experimental investigation of the
533 effects of direct water injection parameters on engine performance in a six-stroke engine. *Energy
534 Convers Manage.* 98 (2015) 89-97.
- 535 [14] A. Kuztalan, Y. Yao, D. Marchant, Y. Wang. A review of novel turbocharger concepts for
536 enhancements in energy efficiency. *Int J of Thermal & Environmental Engineering.* 2 (2011) 75-82.
- 537 [15] A.J. Feneley, A. Pesiridis, A.M. Andwari. Variable Geometry Turbocharger Technologies for
538 Exhaust Energy Recovery and Boosting-A Review. *Renewable and Sustainable Energy Reviews.* 71

539 (2017) 959-75.

540 [16] G. Zamboni, S. Moggia, M. Capobianco. Effects of a Dual-Loop Exhaust Gas Recirculation
541 System and Variable Nozzle Turbine Control on the Operating Parameters of an Automotive Diesel
542 Engine. *Energies*. 10 (2017) 47.

543 [17] X. Shi, T. Wang, C. Ma. Simulations of the diesel engine performance with a two-stage
544 sequential turbocharging system at different altitudes. *Proc Inst Mech Eng Pt D: J Automobile Eng.*
545 228 (2014) 1718-26.

546 [18] B. Zhao, M. Qi, H. Sun, X. Shi. Variable nozzle turbocharger turbine performance
547 improvement and shock wave alternation by distributing nozzle endwall clearances. *Proc Inst Mech*
548 *Eng Pt D: J Automobile Eng.* (2018) 0954407018757620.

549 [19] X. Hou, H. Zhang, F. Yu, H. Liu, F. Yang, Y. Xu, et al. Free piston expander-linear generator
550 used for organic Rankine cycle waste heat recovery system. *ApEn*. 208 (2017) 1297-307.

551 [20] X. Hou, H. Zhang, Y. Xu, F. Yu, T. Zhao, Y. Tian. External load resistance effect on the free
552 piston expander-linear generator for organic Rankine cycle waste heat recovery system. *ApEn*. 212
553 (2018) 1252-61.

554 [21] J. Song, C.-w. Gu. Performance analysis of a dual-loop organic Rankine cycle (ORC) system
555 with wet steam expansion for engine waste heat recovery. *ApEn*. 156 (2015) 280-9.

556 [22] T. Guo, H. Wang, S. Zhang. Comparative analysis of CO₂-based transcritical Rankine cycle
557 and HFC245fa-based subcritical organic Rankine cycle using low-temperature geothermal source.
558 *Science China Technological Sciences*. 53 (2010) 1638-46.

559 [23] A. Boretti. Recovery of exhaust and coolant heat with R245fa organic Rankine cycles in a
560 hybrid passenger car with a naturally aspirated gasoline engine. *Appl Therm Eng*. 36 (2012) 73-7.

561 [24] G. Shu, L. Shi, H. Tian, X. Li, G. Huang, L. Chang. An improved CO₂-based transcritical
562 Rankine cycle (CTRC) used for engine waste heat recovery. *ApEn*. 176 (2016) 171-82.

563 [25] R. Zhao, H. Zhang, S. Song, Y. Tian, Y. Yang, Y. Liu. Integrated simulation and control strategy
564 of the diesel engine–organic Rankine cycle (ORC) combined system. *Energy Convers Manage*. 156
565 (2018) 639-54.

566 [26] M. Jiménez-Arreola, R. Pili, C. Wieland, A. Romagnoli. Analysis and comparison of dynamic
567 behavior of heat exchangers for direct evaporation in ORC waste heat recovery applications from
568 fluctuating sources. *ApEn*. 216 (2018) 724-40.

569 [27] R. Cipollone, D.D. Battista, A. Gualtieri. A novel engine cooling system with two circuits

570 operating at different temperatures. *Energy Conversion & Management*. 75 (2013) 581-92.

571 [28] T. Castiglione, S. Bova, M. Belli. A Model Predictive Controller for the Cooling System of
572 Internal Combustion Engines. *Energy Procedia*. 101 (2016) 582-9.

573 [29] M. Chanfreau, B. Gessier, A. Farkh, P.Y. Geels. The need for an electrical water valve in a
574 THERmal management intelligent system (THEMIS™). SAE Technical Paper2003.

575 [30] M. Gumus. Reducing cold-start emission from internal combustion engines by means of
576 thermal energy storage system. *Appl Therm Eng*. 29 (2009) 652-60.

577 [31] Q.-h. Luo, B.-g. Sun. Experiments on the effect of engine speed, load, equivalence ratio, spark
578 timing and coolant temperature on the energy balance of a turbocharged hydrogen engine. *Energy*
579 *Convers Manage*. 162 (2018) 1-12.

580 [32] C.D. Rakopoulos, E.G. Giakoumis. Second-law analyses applied to internal combustion
581 engines operation. *PrECS*. 32 (2006) 2-47.

582 [33] L. Yingjian, Q. Qi, H. Xiangzhu, L. Jiezhi. Energy balance and efficiency analysis for power
583 generation in internal combustion engine sets using biogas. *Sustainable energy technologies and*
584 *assessments*. 6 (2014) 25-33.

585 [34] A. Gharehghani, M. Koochak, M. Mirsalim, T. Yusaf. Experimental investigation of thermal
586 balance of a turbocharged SI engine operating on natural gas. *Appl Therm Eng*. 60 (2013) 200-7.

587 [35] M. Abedin, H. Masjuki, M. Kalam, A. Sanjid, S.A. Rahman, B. Masum. Energy balance of
588 internal combustion engines using alternative fuels. *Renewable and Sustainable Energy Reviews*.
589 26 (2013) 20-33.

590 [36] <https://bbs.360che.com/thread-814849-1-1.html>.

591 [37] <http://www.doc88.com/p-1983438979559.html>.

592 [38] D. Jung, J. Yong, H. Choi, H. Song, K. Min. Analysis of engine temperature and energy flow in
593 diesel engine using engine thermal management. *Journal of Mechanical Science and Technology*. 27
594 (2013) 583-92.

595 [39] A. Torregrosa, A. Broatch, P. Olmeda, C. Romero. Assessment of the influence of different
596 cooling system configurations on engine warm-up, emissions and fuel consumption. *International*
597 *Journal of Automotive Technology*. 9 (2008) 447-58.

598 [40] T. Castiglione, S. Bova, M. Belli. A Novel Approach to the Thermal Management of Internal
599 Combustion Engines. *Energy Procedia*. 126 (2017) 883-90.

600 [41] X. Lei, M. Qi, H. Sun, X. Shi, L. Hu. Study on the Interaction of Clearance Flow and Shock

601 Wave in a Turbine Nozzle. SAE Technical Paper2017.

602 [42] M. Qi, M. Zhang, C. Ma. Influences of Dis-tuned Tip Clearance on the Discrete Aerodynamic
603 Noise in Centrifugal Compressor. (2016).

604 [43] M. Qi, X. Lei, Z. Wang, C. Ma. Investigation on the flow characteristics of a VNT turbine
605 under pulsating flow conditions. Proc Inst Mech Eng Pt D: J Automobile Eng. (2017)
606 0954407017744922.

607 [44] C.A. Rinaldini, S. Breda, S. Fontanesi, T. Savioli. Two-Stage turbocharging for the downsizing
608 of SI V-Engines. Energy Procedia. 81 (2015) 715-22.

609 [45] R. Liu, Z. Zhang, S. Dong, G. Zhou. High-Altitude Matching Characteristic of Regulated
610 Two-Stage Turbocharger With Diesel Engine. Journal of Engineering for Gas Turbines and Power.
611 139 (2017) 094501.

612 [46] F. Yang, X. Dong, H. Zhang, Z. Wang, K. Yang, J. Zhang, et al. Performance analysis of waste
613 heat recovery with a dual loop organic Rankine cycle (ORC) system for diesel engine under various
614 operating conditions. Energy Convers Manage. 80 (2014) 243-55.

615 [47] F. Yang, H. Zhang, C. Bei, S. Song, E. Wang. Parametric optimization and performance
616 analysis of ORC (organic Rankine cycle) for diesel engine waste heat recovery with a fin-and-tube
617 evaporator. Energy. 91 (2015) 128-41.

618 [48] F. Yang, H. Zhang, Z. Yu, E. Wang, F. Meng, H. Liu, et al. Parametric optimization and heat
619 transfer analysis of a dual loop ORC (organic Rankine cycle) system for CNG engine waste heat
620 recovery. Energy. 118 (2017) 753-75.

621 [49] X. Li, G. Shu, H. Tian, L. Shi, X. Wang. Dynamic Modeling of CO₂ Transcritical Power
622 Cycle for Waste Heat Recovery of Gasoline Engines. Energy Procedia. 105 (2017) 1576-81.

623 [50] L. Shi, G. Shu, H. Tian, G. Huang, T. Chen, X. Li, et al. Experimental comparison between
624 four CO₂-based transcritical Rankine cycle (CTRC) systems for engine waste heat recovery. Energy
625 Convers Manage. 150 (2017) 159-71.

626 [51] S.-s. Wang, C. Wu, J. Li. Exergoeconomic analysis and optimization of single-pressure
627 single-stage and multi-stage CO₂ transcritical power cycles for engine waste heat recovery: A
628 comparative study. Energy. (2017).

629 [52] C. Ma, J. Gao, L. Zhong, S. Xing. Experimental investigation of the oxidation behaviour and
630 thermal kinetics of diesel particulate matter with non-thermal plasma. Appl Therm Eng. 99 (2016)
631 1110-8.

632 [53] J. Gao, C. Ma, S. Xing, L. Sun. Oxidation behaviours of particulate matter emitted by a diesel
633 engine equipped with a NTP device. *Appl Therm Eng.* 119 (2017) 593-602.

634 [54] J. Gao, C. Ma, S. Xing, L. Sun, L. Huang. A review of fundamental factors affecting diesel PM
635 oxidation behaviors. *Science China Technological Sciences.* 61 (2018) 330–45.

636 [55] J. Gao, G. Tian, A. Sorniotti, A.E. Karci, R. Di Palo. Review of thermal management of
637 catalytic converters to decrease engine emissions during cold start and warm up. *Appl Therm Eng.*
638 147 (2019) 177-87.

639 [56] J.T.B.A. Kessels, D.L. Foster, W.A.J. Bleuanus. Fuel Penalty Comparison for (Electrically)
640 Heated Catalyst Technology Comparaison. *Oil & Gas Science & Technology.* 65 (2010) 47-54.

641 [57] T. Ma, N. Collings, T. Hands. Exhaust Gas Ignition (EGI) - A New Concept for Rapid
642 Light-Off of Automotive Exhaust Catalyst. *International Congress & Exposition1992.*

643 [58] W. Maus, R. Brück, R. Konieczny, A. Scheeder. Electrically heated catalyst for thermal
644 management in modern vehicle applications. *Mtz Worldwide.* 71 (2010) 34-9.

645 [59] P. Kauranen, T. Elonen, L. Wikström, J. Heikkinen, J. Laurikko. Temperature optimisation of a
646 diesel engine using exhaust gas heat recovery and thermal energy storage (diesel engine with
647 thermal energy storage). *Appl Therm Eng.* 30 (2010) 631-8.

648 [60] D.J. Allen, M.P. Lasecki. Thermal management evolution and controlled coolant flow. *SAE*
649 *technical paper2001.*

650 [61] H. Kang, H. Ahn, K. Min. Smart cooling system of the double loop coolant structure with
651 engine thermal management modeling. *Appl Therm Eng.* 79 (2015) 124-31.

652 [62] D. Chalet, M. Lesage, M. Cormerais, T. Marimbordes. Nodal modelling for advanced
653 thermal-management of internal combustion engine. *ApEn.* 190 (2017) 99-113.

654 [63] A.K. Haghghat, S. Roumi, N. Madani, D. Bahmanpour, M.G. Olsen. An intelligent cooling
655 system and control model for improved engine thermal management. *Appl Therm Eng.* 128 (2018)
656 253-63.

657 [64] M. André. In *Actual Use Car Testing: 70,000 Kilometers and 10,000 Trips by 55 French Cars*
658 *under Real Conditions. International Congress & Exposition1991.*

659 [65] F. Will, A. Boretti. A New Method to Warm Up Lubricating Oil to Improve the Fuel Efficiency
660 During Cold Start. *Sae International Journal of Engines.* 4 (2011) 175-87.

661 [66] A. Roberts, R. Brooks, P. Shipway. Internal combustion engine cold-start efficiency: A review
662 of the problem, causes and potential solutions. *Energy Convers Manage.* 82 (2014) 327-50.

663 [67] I. Shancita, H. Masjuki, M. Kalam, I.R. Fattah, M. Rashed, H. Rashedul. A review on idling
664 reduction strategies to improve fuel economy and reduce exhaust emissions of transport vehicles.
665 Energy Convers Manage. 88 (2014) 794-807.

666